ACS Photonics

Letter

pubs.acs.org/journal/apchd5

Vector Vortex Beam Generation with a Single Plasmonic Metasurface

Fuyong Yue,[†,⊥] Dandan Wen,[†,⊥] Jingtao Xin,[‡] Brian D. Gerardot,[†] Jensen Li,[§] and Xianzhong Chen*[,†]

[†]SUPA, Institute of Photonics and Quantum Sciences, School of Engineering and Physical Sciences, Heriot-Watt University, Edinburgh, EH14 4AS, U.K.

[‡]Beijing Engineering Research Centre of Optoelectronic Information and Instruments, Beijing Information Science and Technology University, Beijing, 100192, China

[§]School of Physics and Astronomy, University of Birmingham, Birmingham, B15 2TT, U.K.

Supporting Information

ABSTRACT: Despite a plethora of applications ranging from quantum memories to high-resolution lithography, the current technologies to generate vector vortex beams (VVBs) suffer from less efficient energy use, poor resolution, low damage threshold, and bulky size, preventing further practical applications. We propose and experimentally demonstrate an approach to generate VVBs with a single metasurface by locally tailoring phase and transverse polarization distribution. This method features the spin−orbit coupling and the superposition of the converted part with an additional phase pickup and the residual part without a phase change. By maintaining the equal components for the converted part and the residual part, the cylindrically polarized vortex beams carrying orbital angular momentum are experimentally demonstrated based on a single metasurface at subwavelength scale. The proposed approach provides unprecedented freedom in engineering the properties of optical waves with high-efficiency light utilization and a minimal footprint.

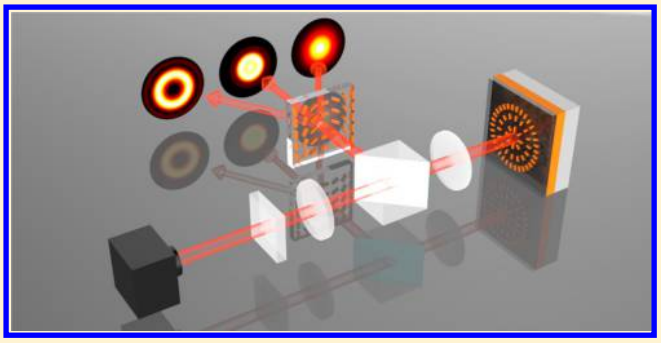

KEYWORDS: *metasurface, vector vortex beam, orbital angular momentum, inhomogeneous polarization distribution*

Structured beams such as vortex beams (VBs) and vector vortex beams (VVBs) have been widely investigated as new promising resources due to the extra degree of freedom for light manipulation. VBs have a distribution of azimuthal phase and homogeneous polarization, while VVBs have an inhomogeneous polarization distribution (such as radial polarization) in the transverse plane and also carry orbital angular momentum. The applications of structured beams have been found in quantum memories,[1] particle trapping,[2] optical communication,[3,4] and high-resolution lithography.[5−8] A radially polarized beam, for example, can be focused more sharply and give rise to a centered longitudinal field, paving the way to higher resolution lithography and optical sensing. An azimuthally polarized beam with a helical phase front, which carries an orbital angular momentum, can effectively achieve a significantly smaller spot size in comparison with that for a radially polarized beam with a planar wavefront in a higher-NA condition. Many approaches and methods, including liquid-crystal q-plates,[9,10] a spatial light modulator, and optical elements using femtosecond laser direct writing technology,[11] have been proposed to generate vector vortex beams. However, these systems could not be straightforwardly downsized, preventing widespread applications in integrated optics. In addition, the limitations of poor resolution and low damage threshold still need to be overcome for practical applications. There are numerous challenges, either fundamental or technological, in building devices that are compact, efficient, and integrable.

Optical metasurfaces, ultrathin inhomogeneous media with planar structures of nanopatterns that manipulate the optical properties of light at the subwavelength scale, have become a current subject of intense research due to the unprecedented control of light propagation. Metasurfaces have been widely used in many exotic research areas, including the photonic spin Hall effect,[12] invisibility cloaking,[13] lensing,[14−18] and holography.[19,20] Especially, geometric metasurfaces, regarded functionally as Pancharatnam−Berry phase optical elements,[21,22] are one of the most exciting recent advances in nano-optics due to their capability of tailoring the field of the emerging beams into nontrivial structures based on optical spin−orbit interactions.[23,24] Geometric metasurfaces have been reported to realize orbital angular momentum generation.[25−28] However, the conversion efficiency is limited, and only the converted part with an additional phase pickup is used. Consequently, various methods to improve the conversion efficiency of plasmonic metasurface are investigated, such as catenary metsurfaces,[29,30] hybrid bilayer metasurfaces,[31] planarized metasurface stacks,[32] and monolayer reflective metasurfaces. Nevertheless, the polarization distribution of the beam is still homogeneous

Received: June 13, 2016
Published: July 20, 2016

DOI: 10.1021/acsphotonics.6b00392
ACS Photonics 2016, 3, 1558−1563

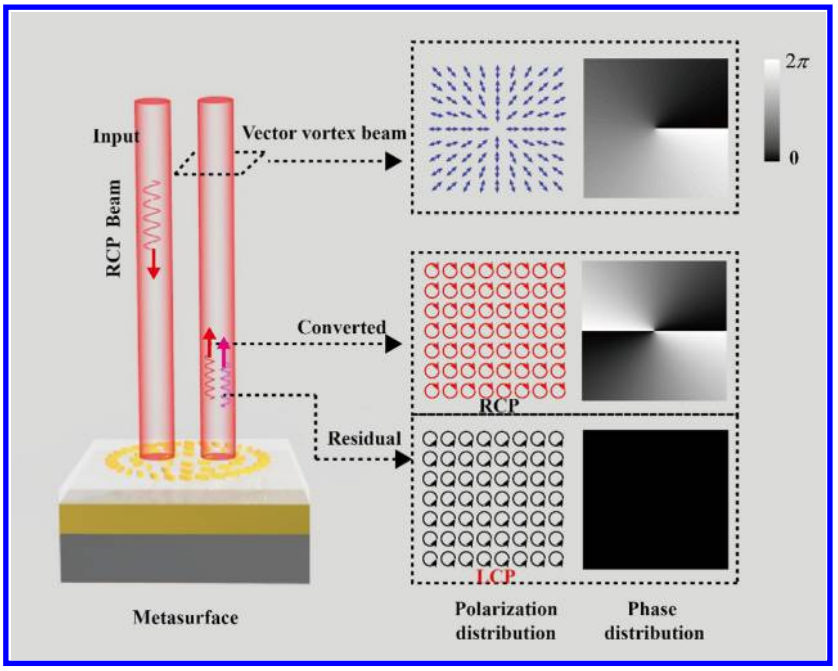

Figure 1. Schematic of the vector vortex beam generation through a metasurface and the polarization and phase distributions of the generated beams. The resultant beam is a superposition of the converted part and the residual part. The converted part has the same circular polarization as that of the incident beam and an additional phase pickup, while the residual part has opposite helicity but no phase change. Upon illumination of RCP light, the converted beam has a helical wavefront with a topological charge of $l = 2$, and the resultant beam has radial polarization distribution with the OAM of $l = 1$. A light beam with azimuthal polarization and flipped sign of the OAM will be generated when changing the polarization state of incident light from RCP to LCP.

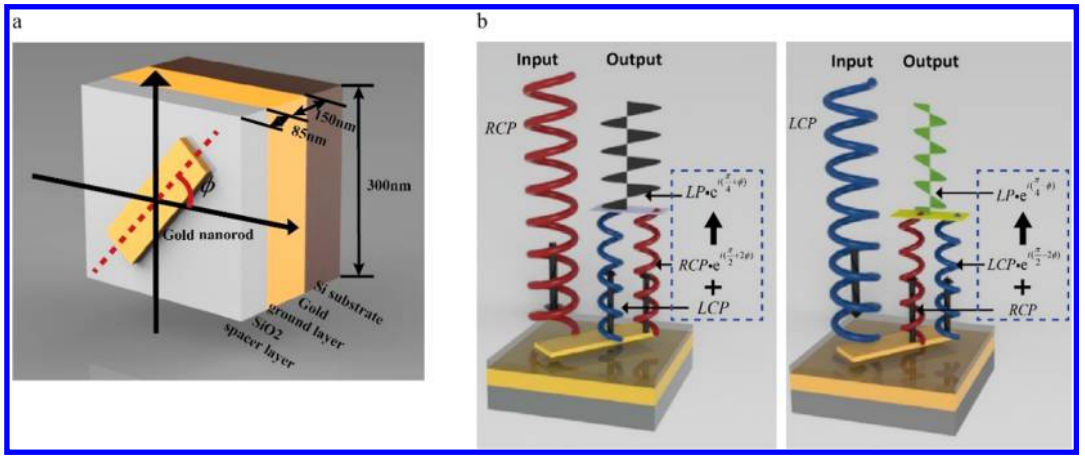

Figure 2. Illustration of the single-pixel cell structure and the polarization conversion of the emerging light. (a) The reflective-type half-wave plate consists of three layers: the ground gold layer (150 nm), the SiO_2 spacer layer (85 nm), and the top layer of gold nanorods (30 nm). Each pixel size is 300 nm by 300 nm. Each nanorod is 200 nm in length, 90 nm in width, and 30 nm in thickness. (b) For the circularly polarized incident light, the emerging light is the superposition of two orthogonal circularly polarized beams corresponding to the converted part (same helicity as the incident beam) and residual part (opposite helicity of the incident beam), respectively. When the converted part and the residual part have equal components, the output beam gives rise to the linearly polarized light. Spiral curves in red color stand for right-handed circularly polarized light (RCP) and those in blue stand for left-handed circularly polarized light (LCP).

since all the functionalities are limited to the phase control. Although one possible solution is to employ two cascaded metasurfaces[33] to generate a structured beam of the vector vortex, the complexity of the required optical system and its large volume sharply affect its performance in system integration and competition capability. Therefore, considering the effective generation of VVBs, an ideal solution is to use a single metasurface to generate these beams carrying an orbital angular momentum with an inhomogeneous polarization distribution.

In this work, we propose and experimentally demonstrate an approach to generate VVBs using a single reflective-type metasurface. The VVBs are generated by using the superposition of the converted part and the residual part of the output beam. The designed metasurfaces to generate cylindrical VVBs carrying orbital angular momentum (OAM) are experimentally demonstrated and characterized. To further validate our proposed approach, a phase-gradient metasurface (PGM) is adopted as a circular polarization beam splitter to decompose the resultant beam. The proposed method opens a

DOI: 10.1021/acsphotonics.6b00392
ACS Photonics 2016, 3, 1558−1563

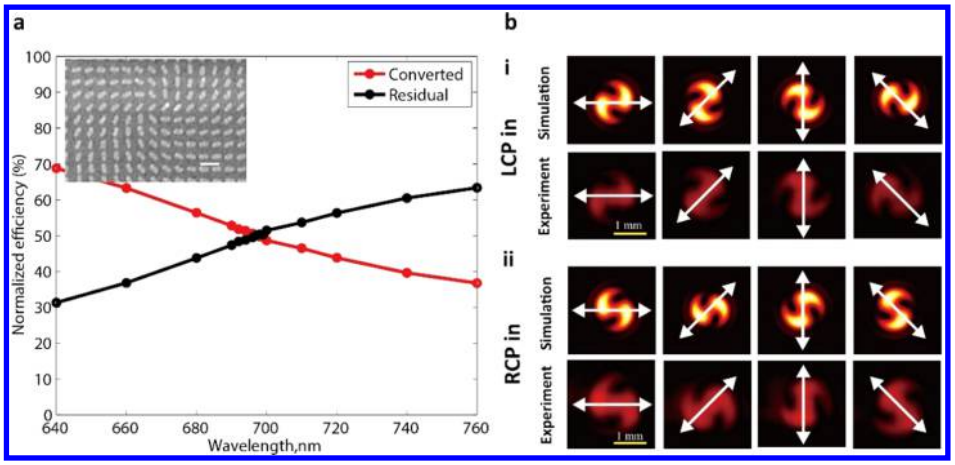

Figure 3. Measured power (normalized) of converted and residual parts at various wavelengths and intensity patterns of a vector vortex beam after passing through a linear polarizer. (a) Measured power (normalized) of converted and residual parts at various wavelengths. The inset is the scanning electron microscopy image of the metasurface for vector vortex beam generation. The scale bar is 500 nm. (b) Simulated and experimentally recorded intensity profile of the vector vortex beam after passing through a polarizer with different polarization angles including horizontal, diagonal, vertical, and antidiagonal directions. The polarization angles are denoted by white double-headed arrows. i, LCP light input, ii, RCP light input.

new window to generate VVBs using a single metasurface, providing new capabilities to develop novel compact devices that may lead to advances in a wide range of fields in optics and photonics.

DESIGN OF THE METASURFACE

Figure 1 shows the schematic of vector vortex beam generation. For an incident light beam, the reflected light from the metasurface consists of two circular polarization states: one has the same handedness as the incident circularly polarized light but with an additional phase delay,[34] and the other has the opposite handedness without the additional phase delay. The additional phase delay is known as a Pancharatnam−Berry phase with a value of $\pm 2\phi$, where ϕ is the orientation angle of each nanorod. Specifically, "+" and "−" represent the sign of the phase shift for the incident RCP light and that for the incident LCP light, respectively. Note that the helicity of polarized light is reversed when it is reflected by an ideal mirror because of the opposite propagation direction. Each pixel size is subwavelength scale. The output beam is therefore a superposition of two components, and thus the polarization distribution is engineered at the nanoscale and transformed to a radial vector field. Upon illumination of RCP (right-handed circularly polarized) light, the generated VVB has a helical wavefront and carries OAM $l = 1$. Furthermore, the polarization distribution is flipped about the vertical axis (see Supplementary Section 1), and the sign of the OAM is reversed when changing the polarization of incident light from RCP to left-handed circular polarization (LCP).

The metasurfaces have the metal−dielectric−metal configuration with the top layer of nanorods with space-variant orientation (Figure 2a). The gold ground layer and SiO_2 spacer layer are deposited on a silicon substrate by electron beam evaporation. The top layer of the nanorods is fabricated using electron-beam lithography and a standard lift-off process, and a 3 nm Ti layer is deposited between the top layer and the SiO_2 spacer layer for adhesion purposes. In previous works, the residual part is minimized and the converted part is maximized when the metasurface functions as a perfect half-wave plate by optimizing the design parameters. To obtain an operating wavelength where the converted and residual part have equal components, we modify the design parameters in ref 19 specifically. For example, in order to target the operating wavelength of 700 nm, we fabricate a series of metasurfaces with all widths of nanorods uniformly biased from their ideal design values in steps of 10 nm. The orientation angles of nanorods are governed by the following expression:

$$\alpha(r, \phi) = \phi + \alpha_0 + \frac{\pi}{4} \tag{1}$$

where (r, ϕ) is the polar coordinate representation. α_0 is the initial angle related to the phase difference of two eigenstates. The additional term $\frac{\pi}{4}$ in eq 1 is explained in the Supplementary Section 2. To clearly illustrate the mechanism, the metasurface is illuminated at normal incidence by an LCP beam with a normalized Jones vector $\frac{1}{\sqrt{2}}\begin{bmatrix}1\\-i\end{bmatrix}$. At a particular location of azimuthal angle ϕ, the polarization state of the resultant beam is generally a superposition of two components with orthogonal circular polarization states, i.e., the converted part with an abrupt phase change, $E_{\mathrm{Con}}^{\mathrm{LCP}}$, and the residual part without phase delay, $E_{\mathrm{Res}}^{\mathrm{LCP}}$. The expression for the superposition is given by

$$\begin{aligned} E_{\mathrm{out}}^{\mathrm{LCP}} &= E_{\mathrm{Con}}^{\mathrm{LCP}} + E_{\mathrm{Res}}^{\mathrm{LCP}} \\ &= \frac{1}{\sqrt{2}}\left(\frac{A}{A+B} e^{i\left(\frac{\pi}{2}-2\phi\right)}\begin{bmatrix}1\\-i\end{bmatrix} + \frac{B}{A+B}\begin{bmatrix}1\\i\end{bmatrix}\right) \end{aligned} \tag{2}$$

Apart from the Ohmic loss and absorption, all of the reflected beams contribute to VVB generation. A and B represent the amplitudes of converted and residual light, respectively. If we tune the reflection properties of the gold nanorods to have $A = B$, the resultant beam gives rise to the linearly polarized light and also acquires a phase change. Its Jones vector is given by

DOI: 10.1021/acsphotonics.6b00392
ACS Photonics 2016, 3, 1558−1563

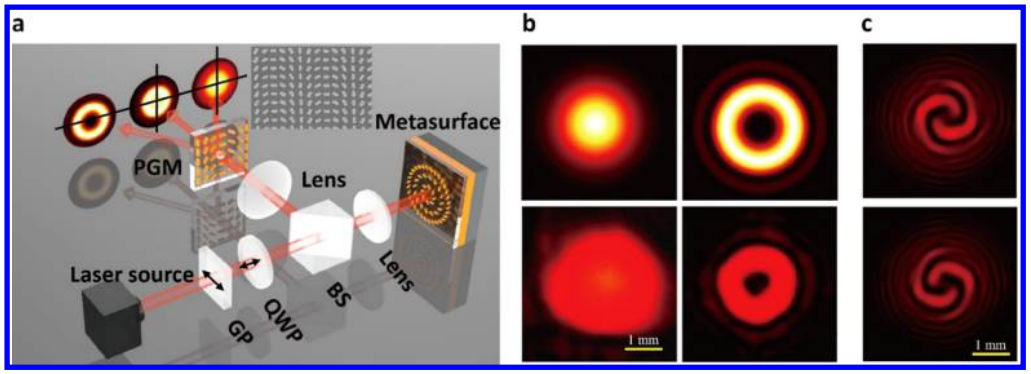

Figure 4. Experimental setup and the theoretically predicted and measured intensity distribution of the two components. (a) Schematic of the experimental setup. The desired circularly polarized light is generated by passing a laser beam (NKT-SuperK EXTREME) through a properly oriented Glan polarizer (GP) and quarter-wave plate (QWP), then normally illuminated upon the metasurface with weak focus. In order to collect the reflected light and project it to a phase-gradient metasurface (PGM), a polarization-insensitive beam splitter (BS) is inserted between the QWP and the lens. A charge coupled device camera is used to image the output beams. The inset is the SEM image of the fabricated phase-gradient metasurface. (b) Simulated (top) and measured (bottom) intensity profiles of the two components. (c) Spiral patterns created by the interference of the vortex beam and a copropagating Gaussian beam. The polarization states of incident light are LCP (upper image) and RCP (lower image), respectively.

$$E_{\text{out}}^{\text{LCP}} = \sqrt{2}\, e^{i\left(\frac{\pi}{4}-\phi\right)} \begin{bmatrix} \cos\left(\frac{\pi}{4}-\phi\right) \\ \sin\left(\frac{\pi}{4}-\phi\right) \end{bmatrix} \tag{3}$$

A similar derivation takes place when the polarization state of the incident light is RCP. The Jones vector of the emerging beam is

$$E_{\text{out}}^{\text{RCP}} = \sqrt{2}\, e^{i\left(\frac{\pi}{4}+\phi\right)} \begin{bmatrix} \cos\left(\frac{\pi}{4}+\phi\right) \\ -\sin\left(\frac{\pi}{4}+\phi\right) \end{bmatrix} \tag{4}$$

The superscripts in eqs 2−4 represent the polarization states of the incident light. Figure 2b shows the polarization and the phase evolution when a circularly polarized incident light is incident upon a metasurface. If $A \neq B$, the resultant beam is elliptically polarized with an additional phase change. More details about polarization and phase evolution can be found in Supplementary Section 1. In brief, our metasurface is able to generate a structured beam from an unstructured one by using spin−orbit coupling. What is more, there is a global phase factor, in the above case $\exp(i(\phi + \pi/4))$, that appears together with the polarization distribution. Therefore, the resultant beam carries orbital angular momentum $l = 1$ as well. The nanorod distribution and polarization distribution of the emerging beam for different α_0 can be found in Figure S2 (Supplementary Section 2).

RESULTS

We design and fabricate two metasurfaces with different values of α_0. For the reflective-type metasurface configuration, the size of the nanorod, the refractive index, the thickness of the spacer layer, and the size of the unit pixel significantly affect the efficiency at a fixed wavelength. Furthermore, the fabrication error (e.g., nanorod distortion and missing nanorods) and the film quality (e.g., cracks) would also lead to the disagreement between the numerical simulation and experiment results. Figure 3a shows the measured normalized power of the two eigenstates over a wide range of wavelengths. The experimental value of Ohmic loss at the resonance frequency of the nanorod is less than 20% for the metal−dielectric−metal configuration. Since our main concern is about the operating wavelength where the converted and nonconverted parts have equal intensities, the two curves for the converted and residual parts are normalized to the sum of these two components. The two curves overlap at the wavelength of 697 nm, which means that the converted and residual part have equal components at this wavelength and the VVB is realized. By passing through a linear polarizer with a different transmission angle, the generated structured beams from the fabricated metasurfaces are characterized and validated. Figure 3b shows the simulated and measured intensity distribution of a vectorial vortex after passing through an analyzing polarizer in horizontal, 45°, vertical, and −45° orientations at a wavelength of 697 nm. The appearance of "s"-shaped patterns is theoretically predicted and experimentally confirmed. The observed patterns indicate that the resultant beams indeed have an inhomogeneous polarization distribution and a helical wavefront. The intensity patterns of vector beams with different OAM can be found in supplementary Figure S3 (Supplementary Section 3). Moreover, the twisted direction of the "s" shape varying with the helicity of the circular polarization is also experimentally confirmed from the obtained intensity patterns.

The vector vortex beam can be considered a superposition of two beams with different circular polarizations, which can be separated by using a phase gradient metasurface (PGM) since different circular polarizations are steered in two directions due to the generated Pancharatnam−Berry phase at the interface. A detailed explanation can be found in Supplementary Section 4. We employ a PGM, without the need of any additional polarizer and waveplate, to simultaneously decompose the output beam from the metasurface. The schematic of the experimental setup is depicted in Figure 4a. Here, the metasurface sample for the VVB generation is mounted on a three-dimensional translation stage and exposed to light from a tunable NKT supercontinuum laser. A Glan polarizer and a quarter-wave plate (QWP) are used to generate the required circularly polarized light. Then the light is weakly focused by a lens with a focal length of 100 mm onto the metasurface to ensure that the beam size is smaller than the sample. In order to

DOI: 10.1021/acsphotonics.6b00392
ACS Photonics 2016, 3, 1558−1563

collect the reflected light, a polarization-insensitive beam splitter is inserted between the QWP and the lens. The reflected vector vortex beam either is projected to the PGM to decompose the resultant beam or propagates in the free space for further application. The SEM image of the PGM is shown in Figure 4a (see inset). The simulated and obtained intensity distributions of two components are shown in Figure 4b. The doughnut shape and singular point confirm the existence of an optical vortex (right in Figure 4b), which corresponds to the converted light. The residual part (left in Figure 4b), on the other hand, is confirmed by the shape without a singularity in the light spot. To further reveal the spiral wavefront and verify the OAM of optical vortex, the PGM is replaced by the circular polarization filter consisting of a quarter-wave plate and a linear polarizer. We deliberately let both the converted and residual beam partially pass the filter by tuning the angle of the quarter-wave plate and linear polarizer. The residual beam serves as the reference spherical wave to interfere with the converted vortex beam. The double-helical intensity profile and the number of branches stemming from the singularity confirm that the converted beam carries an orbital angular momentum of $2\hbar$ (Figure 4c).

DISCUSSION

Efficient generation of the structured optical fields using an ultracompact device has both fundamental and technical importance for photonics-related research. As promising candidates for integrated optics, metasurfaces have opened a broad range of applications for inhomogeneous control amplitude, phase, and polarization of the scattered waves. The proposed method provides an unusual way to generate a vector vortex beam carrying orbital angular momentum using a single metasurface, which will inspire the pursuit of further novel functionalities. To our knowledge, this is the first time that the converted part and the residual part are used together to realize new functionalities to achieve the most efficient light utilization. Both the phase and polarization are manipulated at subwavelength scale by the artificial array of engineered nanorods over the metasurface. On the other hand, both the polarization distribution and the orbital angular momentum of the output wave are controlled by the helicity of the incident light polarization. We develop two metasurfaces with different initial angles ($\alpha_0 = 0$ and $\alpha_0 = \pi$), which can generate radially and azimuthally polarized vortices carrying orbital angular momenta, respectively. The SEM image of the other metasurface with $\alpha_0 = \pi$ and results are available in Figure S5 (Supplementary Section 5). The good agreement between the predicted and experimental results confirms the proposed methodology. It has been reported that azimuthally polarized beams with a helical wavefront could effectively achieve a significantly smaller spot than normal azimuthally polarized beams when focused with a high-numerical-aperture objective.

For the application of free-space communication, the optical vortex has attracted growing attention due to its higher data transmission capacity. However, the atmospheric turbulence strongly affects the properties of the optical vortex when propagating in free space. The existence of the vectorial vortex can be identified with longer propagation distance through the atmosphere than the scalar vortex even with vanishing characteristic vortex structure. By carefully designing the angle distribution of the nanorods, any polarization state can be realized using a single metasurface with circularly polarized incident light. In addition, the angle of the resultant polarization is switchable by controlling the helicity of the circularly polarized incident light.

In summary, we propose and experimentally demonstrate an approach to generate vector vortex beams using a single plasmonic metasurface. The uniqueness of the proposed method lies in the combined action of the Pancharatnam–Berry phase and the superposition of two orthogonal circularly polarized light beams. Both the orbital angular momentum and polarization distribution in the transverse plane about the propagation axis are manipulated by a single metasurface consisting of nanorods with spatially variant orientation. As our work solves several major issues typically associated with VVB generation—poor resolution, low damage threshold, bulky size, and complicated experimental setup—it opens a new window for future practical applications of the structured beams in the relevant research fields such as optical communication, particle trapping, microscopy, and quantum optics.

ASSOCIATED CONTENT

Supporting Information

The Supporting Information is available free of charge on the ACS Publications website at DOI: 10.1021/acsphotonics.6b00392.

Additional information (PDF)

AUTHOR INFORMATION

Corresponding Author

*E-mail: x.chen@hw.ac.uk.

Author Contributions

⊥F. Yue and D. Wen contributed equally to this work.

Notes

The authors declare no competing financial interest.

ACKNOWLEDGMENTS

This work is supported by the Engineering and Physical Sciences Research Council of the United Kingdom (grant ref: EP/M003175/1).

REFERENCES

(1) Parigi, V.; D'Ambrosio, V.; Arnold, C.; Marrucci, L.; Sciarrino, F.; Laurat, J. Storage and retrieval of vector beams of light in a multiple-degree-of-freedom quantum memory. *Nat. Commun.* **2015**, *6*, 7706.

(2) Ng, J.; Lin, Z. F.; Chan, C. T. Theory of Optical Trapping by an Optical Vortex Beam. *Phys. Rev. Lett.* **2010**, *104*, 103601.

(3) D'Ambrosio, V.; Nagali, E.; Walborn, S. P.; Aolita, L.; Slussarenko, S.; Marrucci, L.; Sciarrino, F. Complete experimental toolbox for alignment-free quantum communication. *Nat. Commun.* **2012**, 3.96110.1038/ncomms1951

(4) Vallone, G.; D'Ambrosio, V.; Sponselli, A.; Slussarenko, S.; Marrucci, L.; Sciarrino, F.; Villoresi, P. Free-Space Quantum Key Distribution by Rotation-Invariant Twisted Photons. *Phys. Rev. Lett.* **2014**, *113*.10.1103/PhysRevLett.113.060503

(5) Hao, X. A.; Kuang, C. F.; Wang, T. T.; Liu, X. Phase encoding for sharper focus of the azimuthally polarized beam. *Opt. Lett.* **2010**, *35*, 3928–3930.

(6) Dorn, R.; Quabis, S.; Leuchs, G. Sharper Focus for a Radially Polarized Light Beam. *Phys. Rev. Lett.* **2003**, *91*, 233901.

(7) Kang, M.; Chen, J.; Wang, X. L.; Wang, H. T. Twisted vector field from an inhomogeneous and anisotropic metamaterial. *J. Opt. Soc. Am. B* **2012**, *29*, 572–576.

(8) Bauer, T.; Orlov, S.; Peschel, U.; Banzer, P.; Leuchs, G. Nanointerferometric amplitude and phase reconstruction of tightly focused vector beams. *Nat. Photonics* **2013**, *8*, 23–27.

DOI: 10.1021/acsphotonics.6b00392
ACS Photonics 2016, 3, 1558–1563

(9) Cardano, F.; Karimi, E.; Slussarenko, S.; Marrucci, L.; de Lisio, C.; Santamato, E. Polarization pattern of vector vortex beams generated by q-plates with different topological charges. *Appl. Opt.* **2012**, *51*, C1−C6.
(10) Rumala, Y. S.; Milione, G.; Nguyen, T. A.; Pratavieira, S.; Hossain, Z.; Nolan, D.; Slussarenko, S.; Karimi, E.; Marrucci, L.; Alfano, R. R. Tunable supercontinuum light vector vortex beam generator using a q-plate. *Opt. Lett.* **2013**, *38*, 5083−5086.
(11) Beresna, M.; Gecevicius, M.; Kazansky, P. G.; Gertus, T. Radially polarized optical vortex converter created by femtosecond laser nanostructuring of glass. *Appl. Phys. Lett.* **2011**, *98*, 201101.
(12) Yin, X.; Ye, Z.; Rho, J.; Wang, Y.; Zhang, X. Photonic spin Hall effect at metasurfaces. *Science* **2013**, *339*, 1405−1407.
(13) Ni, X.; Wong, Z. J.; Mrejen, M.; Wang, Y.; Zhang, X. An ultrathin invisibility skin cloak for visible light. *Science* **2015**, *349*, 1310−1314.
(14) Yu, N.; Capasso, F. Flat optics with designer metasurfaces. *Nat. Mater.* **2014**, *13*, 139−150.
(15) Lin, D.; Fan, P.; Hasman, E.; Brongersma, M. L. Dielectric gradient metasurface optical elements. *Science* **2014**, *345*, 298−302.
(16) Chen, X.; Huang, L.; Muhlenbernd, H.; Li, G.; Bai, B.; Tan, Q.; Jin, G.; Qiu, C. W.; Zhang, S.; Zentgraf, T. Dual-polarity plasmonic metalens for visible light. *Nat. Commun.* **2012**, *3*, 1198.
(17) Aieta, F.; Kats, M. A.; Genevet, P.; Capasso, F. Multiwavelength achromatic metasurfaces by dispersive phase compensation. *Science* **2015**, *347*, 1342−1345.
(18) Zhu, W.; Song, Q.; Yan, L.; Zhang, W.; Wu, P. C.; Chin, L. K.; Cai, H.; Tsai, D. P.; Shen, Z. X.; Deng, T. W. A flat lens with tunable phase gradient by using random access reconfigurable metamaterial. *Adv. Mater.* **2015**, *27*, 4739−4743.
(19) Zheng, G. X.; Muhlenbernd, H.; Kenney, M.; Li, G. X.; Zentgraf, T.; Zhang, S. Metasurface holograms reaching 80% efficiency. *Nat. Nanotechnol.* **2015**, *10*, 308−312.
(20) Wen, D.; Yue, F.; Li, G.; Zheng, G.; Chan, K.; Chen, S.; Chen, M.; Li, K. F.; Wong, P. W.; Cheah, K. W.; Yue Bun Pun, E.; Zhang, S.; Chen, X. Helicity multiplexed broadband metasurface holograms. *Nat. Commun.* **2015**, *6*, 8241.
(21) Yirmiyahu, Y.; Niv, A.; Biener, G.; Kleiner, V.; Hasman, E. Vectorial vortex mode transformation for a hollow waveguide using Pancharatnam-Berry phase optical elements. *Opt. Lett.* **2006**, *31*, 3252−3254.
(22) Marrucci, L.; Manzo, C.; Paparo, D. Pancharatnam-Berry phase optical elements for wave front shaping in the visible domain: Switchable helical mode generation. *Appl. Phys. Lett.* **2006**, *88*, 221102.
(23) Cardano, F.; Marrucci, L. Spin-orbit photonics. *Nat. Photonics* **2015**, *9*, 776−778.
(24) Bliokh, K. Y.; Rodriguez-Fortuno, F. J.; Nori, F.; Zayats, A. V. Spin-orbit interactions of light. *Nat. Photonics* **2015**, *9*, 796−808.
(25) Karimi, E.; Schulz, S. A.; De Leon, I.; Qassim, H.; Upham, J.; Boyd, R. W. Generating optical orbital angular momentum at visible wavelengths using a plasmonic metasurface. *Light: Sci. Appl.* **2014**, *3*, e167.
(26) Huang, L.; Chen, X.; Muhlenbernd, H.; Li, G.; Bai, B.; Tan, Q.; Jin, G.; Zentgraf, T.; Zhang, S. Dispersionless phase discontinuities for controlling light propagation. *Nano Lett.* **2012**, *12*, 5750−5755.
(27) Yang, Y. M.; Wang, W. Y.; Moitra, P.; Kravchenko, I. I.; Briggs, D. P.; Valentine, J. Dielectric Meta-Reflectarray for Broadband Linear Polarization Conversion and Optical Vortex Generation. *Nano Lett.* **2014**, *14*, 1394−1399.
(28) Mehmood, M.; Mei, S.; Hussain, S.; Huang, K.; Siew, S.; Zhang, L.; Zhang, T.; Ling, X.; Liu, H.; Teng, J. Visible Frequency Metasurface for Structuring and Spatially Multiplexing Optical Vortices. *Adv. Mater.* **2016**, *28*, 2533.
(29) Pu, M.; Li, X.; Ma, X.; Wang, Y.; Zhao, Z.; Wang, C.; Hu, C.; Gao, P.; Huang, C.; Ren, H. Catenary optics for achromatic generation of perfect optical angular momentum. *Sci. Adv.* **2015**, *1*, e1500396.
(30) Li, X.; Pu, M.; Zhao, Z.; Ma, X.; Jin, J.; Wang, Y.; Gao, P.; Luo, X. Catenary nanostructures as compact Bessel beam generators. *Sci. Rep.* **2016**, *6*.2052410.1038/srep20524
(31) Qin, F.; Ding, L.; Zhang, L.; Monticone, F.; Chum, C. C.; Deng, J.; Mei, S.; Li, Y.; Teng, J.; Hong, M. Hybrid bilayer plasmonic metasurface efficiently manipulates visible light. *Sci. Adv.* **2016**, *2*, e1501168.
(32) Monticone, F.; Estakhri, N. M.; Alù, A. Full control of nanoscale optical transmission with a composite metascreen. *Phys. Rev. Lett.* **2013**, *110*, 203903.
(33) Yi, X. N.; Ling, X. H.; Zhang, Z. Y.; Li, Y.; Zhou, X. X.; Liu, Y. C.; Chen, S. Z.; Luo, H. L.; Wen, S. C. Generation of cylindrical vector vortex beams by two cascaded metasurfaces. *Opt. Express* **2014**, *22*, 17207−17215.
(34) Huang, L.; Chen, X.; Mühlenbernd, H.; Li, G.; Bai, B.; Tan, Q.; Jin, G.; Zentgraf, T.; Zhang, S. Dispersionless phase discontinuities for controlling light propagation. *Nano Lett.* **2012**, *12*, 5750−5755.

DOI: 10.1021/acsphotonics.6b00392
ACS Photonics 2016, 3, 1558−1563